

Formulation of a Monte Carlo model for edge plasma transport

Y. Feng, J. Kisslinger and F. Sardei

Max-Planck-Institut für Plasmaphysik, Euratom Association, D-85748 Garching, Germany

1. Introduction

The Braginskii's fluid equations [1] for particle, momentum and energy can be generalized into a Fokker-Planck form

$$\frac{\partial f}{\partial t} + \nabla \cdot [\mathbf{V}f - \mathbf{D} \cdot \nabla f] = S \quad (1)$$

where $\mathbf{D} = D_{\parallel} \mathbf{b}\mathbf{b} + D_{\perp} (\mathbf{I} - \mathbf{b}\mathbf{b})$ is the diffusion tensor written in the same form as for the so-called CGL pressure tensor [2], with $\mathbf{b} = \mathbf{B}/B$ being the unit vector of the B-field line and \mathbf{I} a unit tensor. The function f stands for density, parallel momentum and ion and electron temperature. \mathbf{V} , D_{\parallel} , D_{\perp} and S represent transport coefficients and source terms specific to a particular meaning of f . Whereas a standard finite-difference method solves a linear matrix for the unknown quantities at global grid points, the Monte Carlo technique applied in the 3D edge transport code EMC3 [3] follows microscopic 'particles' governed by a local transition probability function instead. The transition probability function is derived in a local, field-aligned orthogonal coordinate system in which the diffusion tensor is diagonal and non-trivial metric coefficients disappear, reflecting the independence of the parallel and cross-field transports. In addition, an independent global coordinate system is introduced to define a grid needed for scoring Monte Carlo 'particles' and for representing plasma parameters. This paper is however focussed on discussion of the transport dynamics associated with the magnetic field geometry, rather than a complete description of the EMC3 code.

2. Microscopic transport process

The Fokker-Planck equation originated from describing the Brownian motion of particles. To understand the relation of equation (1) to a microscopic system, we consider a Markoff process in which the probability $f(\mathbf{r}, t+\tau)$ at a later time $t+\tau$ is completely determined by the probability at time t (see e.g. Ref. [4]):

$$f(\mathbf{r}, t+\tau) = \int T(\mathbf{r}, t+\tau | \mathbf{r}', t) f(\mathbf{r}', t) d\mathbf{r}' \quad (2)$$

where $T(\mathbf{r}, t+\tau | \mathbf{r}', t)$ is the transition probability (conditional probability density). A formal Taylor series expansion of equation (2) in τ and $\Delta\mathbf{r} (= \mathbf{r} - \mathbf{r}')$ yields

$$\frac{\partial f}{\partial t} + \nabla \cdot \left[f \frac{1}{\tau} \int \Delta\mathbf{r} T(\mathbf{r} + \Delta\mathbf{r}, t+\tau | \mathbf{r}, t) d\Delta\mathbf{r} - \nabla \cdot \left(f \frac{1}{2\tau} \int \Delta\mathbf{r} \Delta\mathbf{r} T(\mathbf{r} + \Delta\mathbf{r}, t+\tau | \mathbf{r}, t) d\Delta\mathbf{r} \right) \right] = 0. \quad (3)$$

One sees that, in the absence of the source, equation (1) and (3) become identical if we let

$$\frac{1}{\tau} \int \Delta\mathbf{r} T(\mathbf{r} + \Delta\mathbf{r}, t+\tau | \mathbf{r}, t) d\Delta\mathbf{r} = \mathbf{V} + \nabla \cdot \mathbf{D} \quad (4)$$

$$\text{and } \frac{1}{2\tau} \int \Delta\mathbf{r} \Delta\mathbf{r} T(\mathbf{r} + \Delta\mathbf{r}, t+\tau | \mathbf{r}, t) d\Delta\mathbf{r} = \mathbf{D}, \quad (5)$$

implying that equation (1) can be solved in a stochastic way. Equations (4) and (5) relate the macroscopic variables \mathbf{V} and \mathbf{D} to a microscopic stochastic process described by a transition probability $T(\mathbf{r} + \Delta\mathbf{r}, t+\tau | \mathbf{r}, t)$. Notice that all the macroscopic variables f , \mathbf{V} and \mathbf{D} depend only on \mathbf{r} of a macroscopic size and, for a given \mathbf{r} , the transition probability is only a function of $\Delta\mathbf{r}$ which varies in a microscopic range. Therefore, it is reasonable to introduce two independent coordinate systems: a **global** coordinate system \mathbf{r} to define macroscopic variables and a **local** $\Delta\mathbf{r}$ to describe the dynamics of the stochastic process. In the following we restrict our attention to discussion on transport dynamics associated with the local coordinate system.

The stochastic transport mechanisms are described by a transition probability function which can be derived from equations (4) and (5) if a local coordinate system is selected at a given point $P(\mathbf{r})$. According to

$$\nabla \cdot \mathbf{D} = \nabla D_{\perp} + \mathbf{b}\mathbf{b} \cdot \nabla (D_{\parallel} - D_{\perp}) + \mathbf{b}(D_{\parallel} - D_{\perp})\nabla \cdot \mathbf{b} + (D_{\parallel} - D_{\perp})(\mathbf{b} \cdot \nabla)\mathbf{b} \quad (6)$$

it is convenient to use the three orthogonal unit vectors $\mathbf{e}_1 = -(\mathbf{b} \cdot \nabla)\mathbf{b}/|(\mathbf{b} \cdot \nabla)\mathbf{b}|$, $\mathbf{e}_2 = \mathbf{b} \times \mathbf{e}_1$ and \mathbf{b} as a triplet of the local coordinate system, as shown in Fig. 1. In this coordinate system, the transport coefficients read

$$\mathbf{V} + \nabla \cdot \mathbf{D} = \begin{pmatrix} V_{\Delta x} \\ V_{\Delta y} \\ V_{\Delta z} \end{pmatrix} = \begin{pmatrix} \mathbf{e}_1 \cdot (\mathbf{V} + \nabla D_{\perp}) - (D_{\parallel} - D_{\perp})|(\mathbf{b} \cdot \nabla)\mathbf{b}| \\ \mathbf{e}_2 \cdot (\mathbf{V} + \nabla D_{\perp}) \\ \mathbf{b} \cdot (\mathbf{V} + \nabla D_{\parallel}) + (D_{\parallel} - D_{\perp})\nabla \cdot \mathbf{b} \end{pmatrix} \quad (7) \text{ and } \mathbf{D} = \begin{pmatrix} D_{\perp} & 0 & 0 \\ 0 & D_{\perp} & 0 \\ 0 & 0 & D_{\parallel} \end{pmatrix} \quad (8)$$

Use the ansatz

$$T(\Delta x, \Delta y, \Delta z, \tau) = \frac{1}{M \cdot N \cdot L} \sum_{m,n,l} \delta_m(\Delta x - \Delta x_m) \delta_n(\Delta y - \Delta y_n) \delta_l(\Delta z - \Delta z_l) \quad (9)$$

and insert equations (7), (8) and (9) into equations (4) and (5). Integration of equations (4) and (5) yields six relevant equations since the non-diagonal terms in integral (5) linear in τ vanish automatically in the orthogonal coordinates. It is found that solutions of these equations exist only for $M, N, L \geq 2$. For the simplest case with $M=N=L=2$, we have

$$\begin{cases} \Delta x_{1,2} = V_{\Delta x} \tau \pm \sqrt{2D_{\perp} \tau} \\ \Delta y_{1,2} = V_{\Delta y} \tau \pm \sqrt{2D_{\perp} \tau} \\ \Delta z_{1,2} = V_{\Delta z} \tau \pm \sqrt{2D_{\parallel} \tau} \end{cases} \quad (10).$$

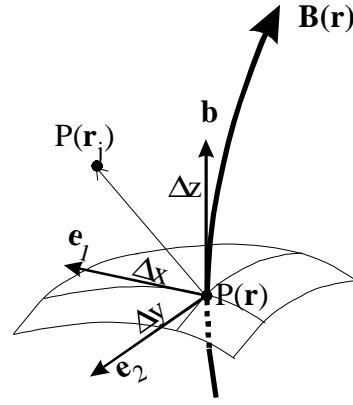


Fig. 1: Local orthogonal coordinate system

3. Monte Carlo simulation

Let f represent the density of particles which undergo convective and diffusive processes in a system of a macroscopic size. The transport domain is covered by a global mesh consisting of a finite number of cells of arbitrary form. Each cell has a non-zero volume Δv_i where the index i indicates the cell number. Assume that each particle at time t can be identified by a δ -function $\delta_j(\mathbf{r} - \mathbf{r}_j(t))$ where $\mathbf{r}_j(t)$ is the location of the j -th particle. After a small time step τ , particles are to be found at new positions $\mathbf{r}_j(t+\tau)$ due to the displacements described by equations (9) and (10). Now, we introduce the independent random variables ξ_x , ξ_y and ξ_z . Each of them has only two discrete values -1 and $+1$. Thus, equation (10) can be rewritten as

According to equation (9), ξ_x , ξ_y and ξ_z are assigned either -1 or $+1$ with equal probability $1/2$,

$$\Delta x(\xi_x) = V_{\Delta x} \tau + \xi_x \sqrt{2D_{\perp} \tau}, \quad \Delta y(\xi_y) = V_{\Delta y} \tau + \xi_y \sqrt{2D_{\perp} \tau}, \quad \Delta z(\xi_z) = V_{\Delta z} \tau + \xi_z \sqrt{2D_{\parallel} \tau}. \quad (11)$$

leading to a random walk of particles. Without specification of boundary conditions (assume that no particles at time $t+\tau$ can reach a boundary), the position of the j -th particle at time $t+\tau$ is determined by

$$\mathbf{r}_j(t+\tau) = \mathbf{r}_j(t) + \Delta x(\xi_x) \mathbf{e}_1 + \Delta y(\xi_y) \mathbf{e}_2 + \Delta z(\xi_z) \mathbf{b}. \quad (12)$$

Through equation (12) we can locate the positions of individual particles at any later time points $t+n\tau$. If the number of the followed particles is large enough such that at any time points $t+n\tau$ each cell is filled by a sufficient amount of particles, the density f is simply given by

$$f(\Delta v_i, t+n\tau) = \frac{1}{\Delta v_i} \sum_j \int_{\Delta v} w_j(t+n\tau) \delta_j[\mathbf{r} - \mathbf{r}_j(t+n\tau)] d\mathbf{r} \quad (13)$$

where $w_j(t+n\tau)$ is the weight of the j -th particle at time $t+n\tau$.

Equations (12) and (13) are given in general forms without any specifications for the global coordinates because the stochastic process happens in a local independent coordinate system. The displacements are then mapped onto a global coordinate system through three basis vectors which are completely determined by the B-field geometry. In order well to understand the stochastic processes associated with the curvature of B-field lines, we consider a simple case in which particles diffuse along a flux tube ($\mathbf{V} = 0$, $D_{\perp} = 0$). We assume that the particles have been reached a steady-state and are source-free in the region of interest. In the following we derive the net flux of the microscopic particles through the cross-section S_0 at L_0 (see Fig. 2). For this simple case, the transition probability function (9) consists, according to (10), of only two discrete points, i.e., $\mathbf{r}_{1,2} = \mathbf{r} + [V_{\Delta z}\tau \pm (2D_{\parallel}\tau)^{1/2}] \mathbf{b} + V_{\Delta x}\tau \mathbf{e}_1$ where \mathbf{r} is the initial position of a particle as shown in Fig. 2. It can be shown that, for a small τ ($V_{\Delta z}\tau \ll (2D_{\parallel}\tau)^{1/2}$) and an expansion of the B-field

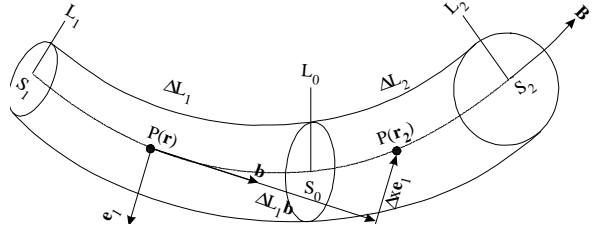


Fig.2: Parallel diffusive process along a flux tube associated with the curvature of B-field lines.

line at $P(\mathbf{r})$ up to the second derivative, the two points $\mathbf{r}_{1,2}$ do lie on the B-field line passing through $P(\mathbf{r})$, as expected. Thus, the two terms $(2D_{\parallel}\tau)^{1/2} \mathbf{b}$ and $D_{\parallel}\tau(\mathbf{b} \cdot \nabla) \mathbf{b}$ together describe the parallel diffusion. Particles on the both sides of the surface S_0 suffer displacements either in forward or backward direction with equal probability $1/2$. Note that only the half of the particles located in $\Delta L_1 = [(2D_{\parallel}\tau)^{1/2} + V_{\Delta z}\tau]_{l=(L_0+L_1)/2}$ and $\Delta L_2 = [(2D_{\parallel}\tau)^{1/2} - V_{\Delta z}\tau]_{l=(L_0+L_2)/2}$ can pass through the surface S_0 and thereby make contributions to the net flux Γ_{\parallel} . Expanding f , D_{\parallel} and S at L_0 up to their first derivatives, we have

$$\Gamma_{\parallel} = \frac{(f\Delta L_1 S)|_{l=(L_0+L_1)/2} - (f\Delta L_2 S)|_{l=(L_0+L_2)/2}}{2S_0\tau} = -D_{\parallel} \frac{\partial f}{\partial l} + V_{\Delta z} f - f \frac{\partial D_{\parallel}}{\partial l} - f \frac{D_{\parallel}}{S_0} \frac{\partial S}{\partial l}. \quad (14)$$

Use equation (7) for $V_{\Delta z}$ and note that $\mathbf{b} \cdot \nabla = \partial/\partial l$ and $\nabla \cdot \mathbf{b} = B\partial(1/B)\partial l = (\partial S/\partial l)/S$ ($\nabla \cdot \mathbf{B} = 0$ and $\mathbf{B} \cdot \mathbf{S} = \text{constant}$ for the flux tube). Finally, we find that the last three terms on the right side of equation (14) cancel exactly, resulting in a correct net flux expected from equation (1).

4. Benchmark with B2

For a simple neutral plasma consisting of a single ion species the B2 [5] and EMC3 code solve almost the same equations, except for the slight simplifications made in the 3D code for the energy balance equations (for example, neglect of the kinetic and viscous contributions). Therefore, it is interesting to see in which degree of accuracy the fluid equations can be treated by the Monte Carlo method.

First, in order to guarantee a 2D orthogonal grid as required by the B2 code, the island SOL geometry is simplified by a 2D slab model (Fig. 3). The SOL has an area of 3×9 (radial \times poloidal) cm^2 , corresponding to the W7-AS islands with a radius of about 3 cm. For simplicity, we ignore the private region. Secondly, we carefully examine the terms included in the equations in both codes in order to ensure that the two codes deal really with identical equations. For this, the kinetic and viscous energy fluxes which do not appear in the 3D code

are simply switched off from the B2 code. Comparison is carried out for a pure hydrogen plasma with a power flux of 200 kW entering the island SOL between the stagnation- and X-points (see Fig. 3). Instead of applying EIRENE code [6] to determine the particle source S_p , a simple exponential function with a radial and poloidal decay length of 2 and 3 cm is assumed. The source S_p has a maximum at the position of the target cutting the separatrix. Particles and energy get lost only due to the target. On the left and top boundaries the condition of $V_{||} = 0$ is set for the momentum transport due to the island symmetry. The particle diffusion coefficient D is taken to be $0.5 \text{ m}^2/\text{s}$ and furthermore the relation $\chi_e = \chi_i = 3D$ holds. Calculation starts with the coupled energy transport equations for ions and electrons from the initial conditions of a constant density ($n_e = 2 \times 10^{13} \text{ cm}^{-3}$) and temperatures ($T_i = T_e = 20 \text{ eV}$). Then, T_e and T_i are determined by iterations. With the calculated T_e and T_i and the given S_p , sequential iterations of the particle transport and momentum balance equations yield n_e and $V_{||}$. The results from the two codes are compared in Fig. 3 which shows the poloidal profiles (radially averaged) of T_e , T_i , n_e and Mach number. The comparisons show excellent agreement between the two codes, although they are based on completely different solving algorithms.

5. Summary

The transition probability function which governs the transport dynamics of the Monte Carlo procedure used in the EMC3 code is derived in a local, field-aligned orthogonal coordinate system in which the diffusion tensor has a diagonal form and non-trivial metric coefficients disappear. The particle tracing procedure is formulated in a general form, independent of the global coordinates selected. The transport properties associated with non-uniform transport coefficients and the curvature of B-field lines are discussed in details. It is shown that the microscopic processes described by the transition probability function give rise to a correct macroscopic flux. Comparison of EMC3 with B2 shows excellent agreement in spite of the completely different solving algorithms.

References

- [1] S. I. Braginskii, Reviews of Plasma Physics, Vol.1, ed. by M.A. Leontovich, Consultants Bureau, New York (1965) p.205.
- [2] R. D. Hazeltine, J. D. Meiss, *Plasma Confinement* (Addison-Wessley, Redwood City) (1992).
- [3] Y. Feng et al., J. Nucl. Mater. 266-269 (1999) 812.
- [4] H. Risken, *The Fokker-Planck Equation*, (Springer series) (1989).
- [5] B.J. Braams, Ph.D. Thesis, Rijksuniversiteit Utrecht (1986).
- [6] D. Reiter, Jülich Report 1947, Jülich (1984).

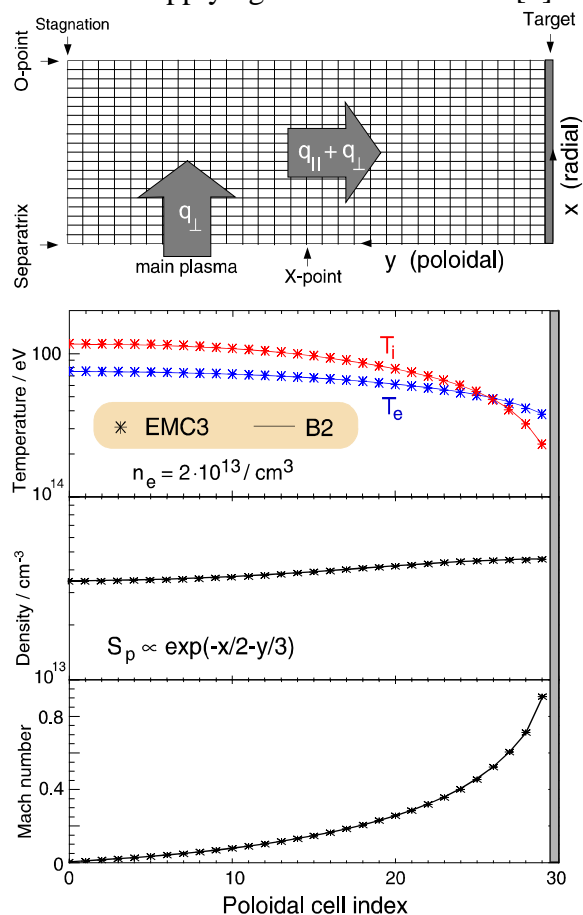


Fig. 3: Comparison of EMC3 with B2, based On a 2D slab model of the island SOL.